On Measurements of Effective Residual Ink Concentration (ERIC) of Deinked Papers Using Kubelka-Munk Theory

D.W. Vahey, J.Y. Zhu and C.J. Houtman

ABSTRACT

The measurement of effective residual ink concentration (ERIC) in recycled papers depends on their opacity. For opacity less than 97.0%, the method is based on application of the Kubelka-Munk theory to diffuse reflection from papers measured once with a black backing and again with a thick backing ofthe same papers. At opacities above 97.0%, the two reflection values tend to become statistically indistinguishable. Measured ERIC values are undetermined owing to a logarithmic singularity in the defining equation. This is handled by using an approximate value for the Kubelka-Munk scattering coefficient ^{S} to remove the singularity. Even when ERIC values can be measured at opacities close to (but slightly less than) 97%, their uncertainty is amplified by the singularity to the point where predicted coefficients of variation (COV) can exceed 50%. In repeat tests of a sample containing five equivalent handsheets, ERIC values for one specimen ranged from 243 to 871 ppm, even though the average opacity for the sample was an acceptable 94.6%. This renders the test marginally useful as a way to monitor the deinking process. Knowledgeable testers may apply an approximate value for sat all opacities that show high measurement variability. However, a new approach to ERIC avoids both the uncertainty and the approximation by using the measurement of diffuse reflection and transmission in single sheets. The Kubelka-Munk theory is again applied to the data, and there is no change in the meaning of ERIC. The measurement is valid at any opacity for which the percentage transmission through the sheet is accurately determined in the near-infrared spectral region. Coefficients of variation are as low as or lower than those from the accepted ERIC measurement throughout the range of interest. Coefficients ofvariation decrease with increasing opacity to a low of 10% for a sheet having 98.7% opacity and 1106 ppm ERIC. In contrast with the accepted method, the COV is remarkably insensitive to the measured value of the scattering coefficient. The new method promises to he a better way to monitor deinking progress in recycled papers.

KEYWORDS

Absorption, Deinked paper, Diffuse, ERIC, Kubelka Munk, Near infrared, Opacity, Recycling, Reflection, Residual ink, Scattering, Transmission

INTRODUCTION

Ink removal is one of the most important steps in recycling of mixed recovered office paper, old magazines, and old newspapers. Ink removal efficiency of a recycling operation is characterized by the brightness increment of the final paper over that of feed stock. Final paper brightness has been used as a product specification of recycled papers. However, the brightness measure has deficiencies in quantifying ink-removal efficiency and the amount of residual ink in deinked pulp because paper brightness depends on additional factors, such as pulp refining, pressing, calendering, and formation. Jordan and Popson [1]-developed a near-infrared reflectance technique to measure residual ink concentration in paper made of deinked pulp using Kubelka-Munk theory [2]. The technique measures reflectance at an infrared wavelength (~950 nm) from a paper sample over a black backmg, R_0, and reflectance from a thick stack of paper from the same sample, R_∞ . The Kubelka-Munk constant k, the specific absorption coefficient of the sample, can be calculated from the two measured reflectance values, R_0 and R_∞ . It is directly related to the residual ink concentration in the paper sample when measured at a near-infrared wavelength where the absorption from lignin and dyes can be ignored [1]. According to Kubelka [3], the specific absorption coefficient is:

Authors are affiliated with USDA Forest Service, Forest Products Laboratory, One Gifford Pinchot Drive, Madison, WI 53726-2398, USA. dvahey@fs.fed.us, jzhu@fs.fed.us, choutman@fs.fed.us.

$$k = s\frac{(1-R_\infty)^2}{2R_\infty} \quad (1a)$$

where

$$s = \left[\frac{R_\infty}{w(1-R_\infty^2)}\right]\ln\left[\frac{1-R_0R_\infty}{1-R_0/R_\infty}\right] \quad (1b)$$

is the specific scattering coefficient, and w is the grammage. The technique has been adopted by TAPPI as provisional test method T 567 pm-97 [4] to measure effective residual ink concentration (ERIC) of deinked pulp. The technique works fairly well except for the large standard deviations encountered in measuring papers of high opacity resulting from high basis weight, ash content, or ink concentration (high ERIC values). This causes concerns in interlaboratory data comparison [1]. These concerns are magnified through the use of several different kinds of spectrometers to measure ERIC in practice, some of which (like most UV-Vis spectrometers) don't extend into the infrared. Low measurement accuracy for high-ERIC papers occurs primarily because the denominator of the logarithmic function in Equation (1b) approaches zero as R_0/R_∞ approaches unity The condition $R_\infty = R_0$ defines a singular point. In tests of opaque papers, measurements of R_0 and R_∞ become statistically indistinguishable, resulting in an indeterminate value for s in Equation (1b) and forcing the use of an approximate value. This anomaly in ERIC measurements using Kubelka-Munk theory motivates the present study. The objectives of the study are:

1) to analytically and experimentally quantify errors in ERIC measurements resulting from application of the TAPPI provisional test method [4] and

2) to demonstrate a complementary method for ERIC measurements that can be applied to high opacity papers without resorting to an approximate value for s .

Much research work bas been conducted on the subject of deficiencies in Kubelka-Munk theory for measurement of paper optical properties under strong light-absorbing conditions [5–11]. In addition, the Foote effect refers to dependency between the two Kubelka-Munk constants; for instance, the specific scattering coefficient s decreases with an increase in the specific absorption coefficient k [12, 13]. The anomaly in ERIC measurements studied here is not related to either limitation of the Kubelka-Munk theory. In this study, the theory is taken at face value as an integral part of the ERIC method.

METHODOLOGY

In the TAPPI provisional test method [4] for measurements of deinked paper based on the work of Jordan and Popson [1], ERIC is the residual ink concentration determined as the ratio between the specific absorption coefficient, k, of the deinked paper and the absorption coefficient of black ink. k_{ink}. Neglecting the absorption by lignin at infrared wavelengths greater than 950 nm,

$$\text{ERIC} = \frac{k}{k_{ink}} \text{x} 10^6 \text{ (ppm)} \quad (2)$$

where k_{ink} = 10,000 m^2/kg , a default value, and the Kubelka-Munk coefficient k is determined from two reflectance measurements using Equation (1). (For simplicity, Equation (1) will be used to refer jointly to Equations (1a) and(1b).)

We propose to take a different and simple experimental approach to determine the Kubelka-Munk coefficients k and s in this study. This new approach measures reflectance at the incident surface, R, and transmission at the back surface, T, from the same paper sample without back reflectance or remounting. For a paper sample with incident light flux $I(w)$ and reflected light flux $J(w)$ at the light-incident surface ($x = w$, measured in basis weight, Figure 1), differential Kubelka-Munk equations within the paper sample can be written as [2, 3]:

$$\frac{dI}{dx} = s(\frac{k}{s}+1)I - sJ \quad (3a)$$

$$\frac{dJ}{dx} = sI - s(\frac{k}{s}+1)J \quad (3b)$$

For the case where there is no radiation returned to the sample by reflection at the hack surface, i.e., $J(0)=0$, the solution for the light reflected from the incident surface is

$$R = R(w) = \frac{J(w)}{I(w)} = \frac{e^{sbw} - e^{-sbw}}{(a+b)e^{sbw} - (a-b)e^{-sbw}} = \frac{\sinh(sbw)}{a\sinh(sbw) + b\cosh(sbw)} \quad (4)$$

where $a=(k/s+1)$and $b^2=a^2-1$.

Transmission at the back surface is

$$T = T(0) = \frac{I(0)}{I(w)} = \frac{2b}{(a+b)e^{sbw} - (a-b)e^{-sbw}} = \frac{b}{a\sinh(sbw) + b\cosh(sbw)} \quad (5)$$

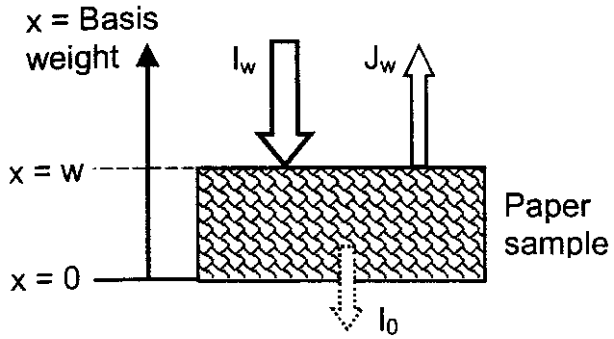

Figure 1. **Geometry for derivation of Kubelka-Munk equations.**

From the ratio of these two equations, the definitions of *a* and *b*, and the hyperbolic identity relation between the cosh and sinh functions, the inverse equations expressing *s* and k in terms of R and Tare found to be:

$$s = \frac{2R}{w\cdot\sqrt{(1-T^2+R^2)^2-4R^2}}\sinh^{-1}\left[\frac{1}{2T}\sqrt{(1-T^2+R^2)^2-4R^2}\right] \quad (6)$$

and

$$k = \frac{(1-R)^2-T^2}{w\cdot\sqrt{(1-T^2+R^2)^2-4R^2}}\sinh^{-1}\left[\frac{1}{2T}\sqrt{(1-T^2+R^2)^2-4R^2}\right] \quad (7)$$

These results agree with Equation (1) and with those of Knox and Wahren [14] when appropriate substitutions are made. A singularity occurs when $T = 0$. The singularity is consistent with that of Equation (1) since a paper for which $T = 0$ must also have $R_0 = R_\infty$. However, when Tis small but finite, differences between R_0 and R_∞ will be on the order of T^2, and therefore much harder to measure accurately than T itself. This translates into greater ERIC measurement accuracy using Equation (7) in place of Equation (1), as will be shown.

Although characterization of optical properties using measurements of R_0 and R_∞ is fairly standard in the paper industry, there are many examples from paper [14], medicine and biology [15−17],paint [18], mineralogy [19, 20], and general instrumentation technology [21] where measurements of *R* and *T* are described. However, this is the first application we know of that applies the measurements to residual ink concentration.

For opacities above 97%, corresponding to *T* less than about 10%, Equation (1) is approximated as

$$k = \bar{s}\left[\frac{(1-R_\infty)^2}{2R_\infty}\right] \quad (8)$$

where $\bar{s}$ is an average value of scattering coefficient based on the idea that scattering should not be expected to change in a sheet as absorption changes. (See, however, the discussion of the interaction between *k* and *s* in the Foote effect [12, 13]). This approach removes the logarithmic singularity in Equation (1) when $R_0 = R_\infty$; however, determination of the best value for $\bar{s}$ in a sampling of recycled newsprints was found to be uncertain by about 10% [1].

ERIC values may be calculated by combining Equation (2) with any of the Equations (7), (1), or (8), depending on the data available. Using the default value $k_{ink} = 10^4$ m²/kg, ERIC(ppm) = 100 k (m²/kg). The three methods for determining ERIC will he referred to as the *RT* method, Equation (7), the R_0R_∞ method, Equation (1), and the $\bar{s}R_\infty$ method, Equation (8).

The main advantage of the *RT* method is that *T* can usually be measured more accurately in absorbing papers than differences between R_0 and R_∞. A secondary advantage is that it only requires measurement of a paper's reflectance at the incident surface and transmittance at the back surface. No sample remounting is required to measure the two properties. The R_0R_∞ method requires measurement of a paper twice to know its properties: first, as a single sheet; second, as part of an opaque stack of paper from the same sample. Remounting is required to perform the test. Because of the inhomogeneity of ink and fiber distribution in paper, the two measurements introduce variability unless perfectly repeated alignment and contact between papers in the stack is maintained from test to test. At high opacities, the precision of the R_0R_∞ method is significantly compromised when the variability in reflectance measurements is amplified by the singularity in Equation (1b).

A disadvantage of the *RT* calculation is that it becomes error prone at low ERIC values for which Equation (7) approximates

$$k \approx \frac{1-R-T}{w} \quad (9)$$

As the numerator becomes small in comparison to the variation in $R + T$, the ERIC coefficient of variation (COV) increases. Therefore, the present technique suffers in measuring low-opacity samples just as the R_0R_∞ method suffers in measuring high-opacity samples. The two techniques are complementary to each other. However, we will see that the superiority of the R_0R_∞ method does not show until ERIC values are below 150 ppm, a value seldom achieved in commercial practice. while the *RT* method works

well from the first stages of ink removal to the commercial range. The $\bar{s}$ R_∞ method is found to be intermediate to the *RT* and R_0R_∞ methods with respect to COV, when reasonable allowance is made for the uncertainty in the estimated scattering coefficient $\bar{s}$ [1].

EXPERIMENTAL

Samples

In this study, five samples consisting of five specimens each were measured for ERIC by the three methods of Equations (7), (1), and (8). Samples were chosen to span a wide range of ERIC values and opacity. Three samples with the highest values were 65 g/m^2 handsheets from a laboratory recycling trial. Recycled thermomechanical pulps with different degrees of residual ink were used. ERIC values were in the range 500 to 1200 ppm. Samples with lower ERIC values (150 to 200 ppm range) included a handsheet from repulped kraft copy paper with residual ink from laser printing, and a commercial newsprint sample of lower basis weight (50 g/m^2). The range of sample opacities was 81.7% to 98.7%.

Each of the bandsheet samples was represented by five specimens, approximately 5 x 6 cm^2, taken from equivalent handsheets. Commercial newsprint specimens were 5 x 5 cm^2 and all came from the same unprinted page of a directory. The handsheet samples had a distinct two-sided roughness associated with the mold that was used. Other differences were minimized to increase sensitivity of experiments to the test method as opposed to within-sample variations.

Testing

The experimental setup is shown in Figure 2. Output from a regulated tungsten halogen lamp (Intralux 6000, Volpi Mfg. Co., Auburn, New York) was collimated using an aperture placed near the focal point of a condenser lens, then chopped, passed through a second aperture, and normally incident on a specimen or stack of five specimens, depending on the experiment. Diameter of the light beam at the sample was approximately 2.1 cm. Light reflected at 45 degrees to the beam axis was incident on a photodiode detector covered with a 25-nm bandpass filter centered at 850 nm wavelength. The photodiode was 1.1 cm in diameter, and the distance of the photodiode from the center of the light spot on the sample was 6 cm. No lens was used between the sample and detector. The signal from the photodiode was amplified and measured on an oscilloscope (Tektronix Model 2247A; Tektronix Inc., Beaverton, Oregon) with voltmeter capabilities. Chopping the light beam allowed peak-to-peak voltage measurements to he made without interference from ambient light.

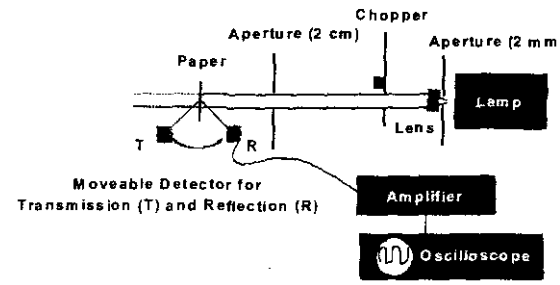

Figure 2. **Experimental arrangement for measurement of paper reflection and transmission.**

The measurement made with this configuration was, after calibration, taken to represent the amount of reflected light *R* used in the calculation for Kubelka-Munk parameters *k* and *s* as given by Equations (6) and (7). The same detector could be quickly repositioned on the output side of the sample to detect transmitted light. For symmetry, it was also positioned at 45 degrees to the optical axis. The calibrated signal in this configuration was taken to represent the transmitted light *T*. *R* and *T* were measured for each sheet. Each of the five sheets in a sample was measured sequentially to complete a test.

For comparison with TAPPI Provisional Measurement T 567 pm-97 [4], reflectance was also measured for a single sheet as described above, with the result designated R_0 instead of *R*. A second measurement was made with the same sheet hacked by four other sheets from the same sample in sequential order of ID. In this case, reflectance was noted as R_∞. Each sheet in the sample was measured to complete a test. All tests were repeated four times at varying delays. Eventually 50 pairs of values represented each sample: five per specimen per test method. In two of the five tests, the non-ID side faced the lamp. This was the smooth side of the handsheet samples. For determination of *k*, averaged values of reflection and transmission measurements were used with the appropriate Equations (1), (7) or (8). With *k* expressed in units of *m^2/kg*, ERIC in *ppm* was 100 x *k*.

In the absence of an integrating sphere, all measured values were based on only a small part of the total light transmitted or reflected by a sample. For the very important calibration, we used a specimen of bleached pulp hoard. The specimen was itself calibrated against a MgO standard used for spectroscopy. The detected signal from the MgO standard at 45 degrees was assumed to represent 100% reflectance. The total reflected and detected signal from the pulp board was less than this by 2.41%, an amount attributed to absorption by the pulp board. The amount of illumination on the sheet in detector volts at any subsequent time was

determined from [$R_{pulpboard}$ (volts) + $T_{pulpboard}$ (volts)]/(1−0.0241). Frequent calibrations to determine this value were performed at the start, the end, and during the sample measurements. Typical illumination of the sample corresponded to 2.5 volts, and the electronic measurement noise was estimated to be about 5 millivolts, or 0.2% of the illumination.

We acknowledge that these experimental methods were developed to make use of equipment on hand rather than equipment optimal for the purpose. We justify this in two ways: first, applicable ERIC values agree well with those determined by Technidyne Corporation (New Albany, Indiana), which manufactures equipment suited to the TAPPI provisional standard [4]. Technidyne used their Master Color Touch instrument to test samples from the trial. Second, the main interest here is in variability of measurements rather than their absolute value. Our approach compromises nuances of design needed for an absolute standard, but not the fundamentals of sample handling, photo detection, and signal processing that are the major sources of variability. The average COV of our measurements for R, R_0 and R_∞ was 4%, and for T was 5%. One to two percent of this variation is attributed to the two-sided differences in the papers.

Other researchers have taken greater efforts to satisfy the requirements of Kubelka-Munk theory with respect to measuring diffuse reflectance and transmittance. Several report the use of single or dual integrating-sphere geometries [15, 17, 18, and 21]. Knox and Wahren [14] developed an instrument specifically suited to studies of opaque paper. It should be considered for future development of the ideas presented here.

Analysis

Table 1 summarizes the three different methods (RT, R_0R_∞, and $\bar{s}\,R_\infty$) of calculating the ERIC value for samples using reflection, transmission, and scattering data. All approaches involve calculating the average of measured reflectance and transmission variables and calculating ERIC from the average. Uncertainty in measurement is determined from the standard deviations of data and the corresponding partial derivatives of the defining equation, as discussed in the Appendix. For each of the three methods, Table 1 references the appropriate equation fork, the Kubelka-Munk absorption coefficient. It also references equations in the Appendix that provide the partial derivatives useful in calculating the uncertainty associated with each method.

Table 1. **Cross reference to equations for calculating ERIC and the ERIC COV.**

Method	ERIC Calculation	ERIC Coefficient of Variation
RT	Equation 7	Equations A1,4-10
R_0R_∞	Equation 1a,b	Equations A2,4,5,11-14
$\bar{s}\,R_\infty$	Equation 8	Equation A3,4,15

RESULTS AND DISCUSSION

Table 2 shows an example of reflection, transmission, and scattering data used in the formulas of Table 1. Data are limited to the second most opaque ofthe five samples tested, with opacity 96.1%. This opacity qualifies for application of the R_0R_∞ method according to the TAPPI provisional standard [4]. Columns representing R, T, R_0 and R_∞ are self-explanatory. Columns representing s show scattering coefficients calculated from individual reflection and transmission data pairs using the R_0R_∞ method (Eq. (1b)) and RT method (Eq. (6)). The column representing $s(R_0,R_\infty)$ has two vacancies where $R_0 \geq R_\infty$. in which cases the values for s and ERIC are undetermined. The RT method, represented by $s(R,T)$ in Table 2, doesn't have any undefined values and therefore should provide a better average value of $\bar{s}$ for use with the $\bar{s}R_\infty$ method. The most opaque sample in the study has opacity $100\,\bar{R}_0/\bar{R}_\infty$=98.7%, and 12 out of 25 of its $s(R_0,R_\infty)$ and ERIC values were

Table 2. **Data and scattering coefficient for the 96.1% opacity sample, Trial 2; i is replicate, j is specimen, bold is 2nd side.**

i,j	R_{ij}	T_{ij}	$(R_0)_{ij}$	$(R_\infty)_{ij}$	$S(R,T)_{ij}$	$S(R_0,R_\infty)_{ij}$
1,1	0.585	0.118	0.537	0.554	49.1	38.7
1,2	0.543	0.117	0.576	0.598	44.1	41.2
1,3	0.570	0.115	0.525	0.570	47.9	28.7
1,4	0.561	0.118	0.545	0.575	46.2	34.0
1,5	0.582	0.094	0.541	0.550	54.4	46.5
2,1	0.598	0.106	0.567	0.611	53.6	33.3
2,2	0.581	0.112	0.557	0.570	49.9	44.5
2,3	0.549	0.115	0.541	0.563	45.4	36.8
2,4	0.561	0.114	0.545	0.572	47.0	35.4
2,5	0.564	0.096	0.534	0.547	51.2	40.9
3,1	0.571	0.108	**0.638**	**0.633**	49.6	
3,2	0.580	0.111	**0.589**	**0.623**	50.0	38.7
3,3	0.533	0.117	**0.600**	**0.608**	43.1	57.1
3,4	0.566	0.116	**0.629**	**0.625**	47.2	
3,5	0.535	0.104	**0.591**	**0.604**	45.8	50.4
4,1	**0.607**	**0.111**	**0.632**	**0.658**	53.6	48.2
4,2	**0.590**	**0.118**	**0.611**	**0.624**	49.8	53.7
4,3	**0.603**	**0.112**	**0.605**	**0.635**	52.8	42.5
4,4	**0.602**	**0.113**	**0.576**	**0.627**	52.4	33.0
4,5	**0.589**	**0.099**	**0.565**	**0.633**	54.1	29.2
5,1	**0.652**	**0.113**	0.543	0.559	59.7	39.6
5,2	**0.590**	**0.125**	0.567	0.606	48.3	34.5
5,3	**0.616**	**0.116**	0.544	0.552	53.9	47.0
5,4	**0.600**	**0.115**	0.569	0.586	51.8	43.0
5,5	**0.607**	**0.097**	0.562	0.579	57.5	42.0
Avg	0.581	0.111	0.572	0.595	50.1	40.4

undetermined. Appropriately, the TAPPI provisional method defaults to the $\bar{s}R_\infty$ method for determining ERIC in this case. No other samples in the study had any undetermined values for s (R_0, R_∞) or ERIC. The possibility of undetermined values is a good reason for averaging reflection and transmission measurements and calculating scattering coefficients from the averages. This has been done in the last row of Table 2.

Table 3 is a summary of average ERIC and s values for each sample as measured by each method, along with the opacity for the samples. Also given are Technidyne values for the trial samples. Technidyne results were determined using the $\bar{s}R_\infty$ method with a constant value for the scattering coefficient, $\bar{s} = 50\ m^2/kg$, consistent with the findings of Jordan and Popson [1]. This is close to the value we measure for the trial samples using R and T data. Results from the R_0R_∞ method also track Technidyne values well. The larger offset reflects the lower value of scattering coefficient measured with this method.

Figure 3 is a plot of ERIC and opacity values from Table 3. Also shown are error bars associated with the use of the *RT* and R_0R_∞ methods. The error bars represent the standard deviation in the results of a single test as determined using relevant equations in the Appendix. Half-error bars are shown to avoid overlap: upward bars refer to the *RT* method. and downward bars refer to the R_0R_∞ method. Error bars associated with the R_0R_∞ method are much larger at high opacity, owing to the singularity in the defining Equation (1). At the highest opacity of 98.7%, the R_0R_∞ method is clearly inappropriate for this reason. However, residual effect ofthe singularity remains at opacity 96.1% (Trial 2). Care must be exercised in using the R_0R_∞ method in the vicinity of 97% opacity. At 94.6% opacity (Trial 1), the error bars for both the *RT* and R_0R_∞ methods are comparable, but the latterproduces a smaller ERIC owing to lower measurements for the scattering coefficient. This tendency of the R_0R_∞ method to produce smaller scattering coefficients than the RT method was observed for all samples. The average reduction was 13%. Better agreement between scattering values calculated from the two methods is reported by Knox and Wahren [14]. However, on their four most opaque samples, values of $\bar{s}$ calculated from R_0R_∞ data were 8% lower than calculated from their version of the *RT* method.

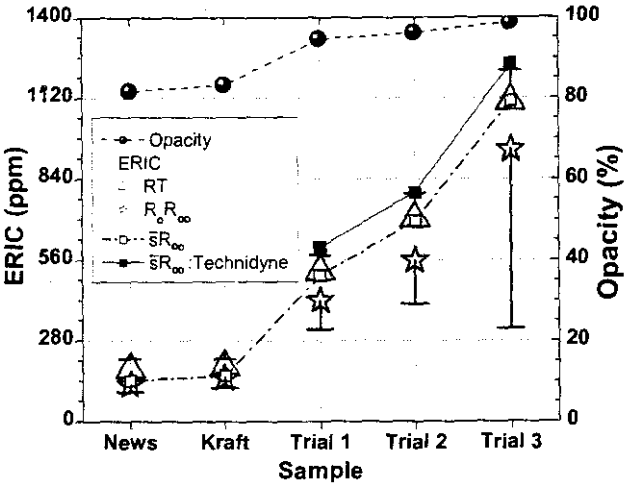

Figure 3. **Effective residual ink concentration (ERIC) measurements using the *RT*, R_0R_∞ and $\bar{s}R_\infty$ methods, contrasted with opacity measurements.**

Figure 4 is a plot of the COV of ERIC as a function of ERIC for all three methods of calculation, based on a precision analysis in the Appendix. Data from Figure 3 are interspersed with theoretical curves. Increasing COV at low ERIC values occurs for all methods, and reflects the decreasing denominator in the COV calculation. The logarithmic format shows the relatively large dependence of COV on scattering coefficient associated with the R_0R_∞ method. In calculating the COV of ERIC for the $\bar{s}R_\infty$ method, we used 10% as the COV of s, inferred from the size of error bars in data by Jordan and Popson [1]. Figure 4 appears to suggest the superiority of the $\bar{s}R_\infty$ method over the R_0R_∞ method for all ERICs above 250 ppm. Jordan and Popson point out the usefulness of the $\bar{s}R_\infty$ method when following process changes on a stable pulp, hut they recommend calculating s for samples from different mills or samples from the same mill when changes in fines and filler content can influence the scattering coefficient [1].

Figure 4 shows that COV based on the R_0R_∞ method is less than that of the *RT* method only for ERIC values less than

Table 3. **ERIC values and Kubelka-Munk scattering coefficients by different methods. The $\bar{s}R_\infty$ method uses S values from the *RT* method.**

		RT Method		R_0R_∞ Method		$\bar{s}R_\infty$ Method		Technidyne	
Sample	Opacity	ERIC	S	ERIC	S	ERIC	S	ERIC	S
News	81.7	181	45.0	127	40.8	140	45.0		
Kraft	83.2	189	30.0	149	28.3	158	30.0		
Trial 1	94.6	519	47.9	417	39.7	504	47.9	602	50.0
Trial 2	96.1	702	50.1	558	40.4	693	50.1	792	50.0
Trial 3	98.7	1106	51.7	939	43.8	1100	51.7	1238	50.0

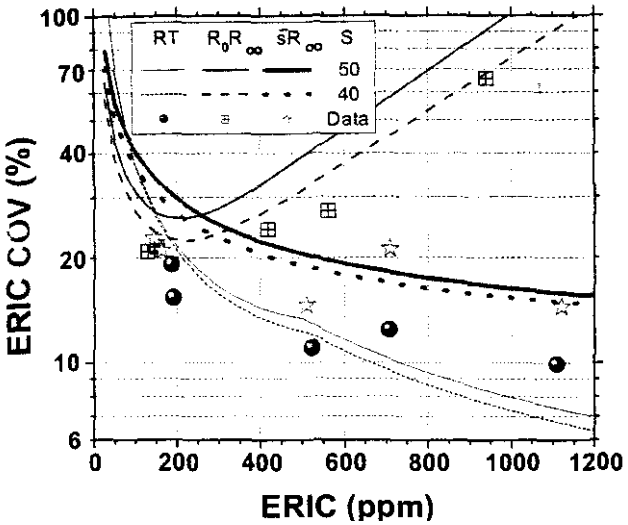

Figure 4. **Coefficient of variation (COV) of effective residual ink concentration (ERIC) values as a function of ERIC.**

150 ppm. As part of a study involving pulp from 27 newsprint deinking lines in 1998, (and 18 lines in 1999). Haynes found that the top quartile of participants produced pulp with an average ERIC value of 235 ppm [22,23]. Although the R_0R_∞ method is comparable in accuracy to the *RT* method at these levels, it appears that commercial deinked pulp is never clean enough to take advantage of the anticipated superiority of the R_0R_∞ method's accuracy at low ERIC levels. The *RT* method is clearly the best choice for monitoring the ink-removal process from start to finish. Over the domain shown in Figure 4, it is even superior to the $\bar{s}R_\infty$ method without the need for use of an approximate value for $\bar{s}$.

When the model used to produce the solid curves in Figure 4 is carried forward to larger ERIC values, the singularity in the *RT* method begins to have an effect. The corresponding ERIC COV first exceeds that of the $\bar{s}R_\infty$ method when ERIC is about 5000 ppm. The estimated opacity at which this happens is 99.999%. The basis for the estimate is the formula for opacity that results from equating the right-hand sides of Equations (6) and (1b) near their singularities $T = 0$ and $R_0 = R_\infty$, respectively. Using the approximation $\sinh^{-1}(x) \cong \ln(2x)$ for large x in Equation (6), we find that the two equations produce equal scattering coefficients when

$$Opacity = 100\% \times \frac{R_0}{R_\infty} = 100\% \times \left(1 - \frac{T^2}{1 - R^2} \right) \quad (10)$$

The modeled values $T = 0.003$ and $R = 0.268$ provide "five-nines" opacity, $s = 50$ m^2/kg, ERIC = 5000 ppm, and ERIC COV = 11%. At this low value for T, the main source of measurement variation is likely to be electronic noise. The model also predicts that the minimum COV associated with the *RT* method is 5% occurring near 2700 ppm ERIC. These large values for ERIC are not likely to be encountered in practice.

SUMMARY AND CONCLUSIONS

The basic functions derived in the Kubelka-Munk theory of two-light-flux propagation in diffusing media are reflection and transmission, R and T. Many authors have used measurements of R and T to solve for inverse variables of absorption k and scattering s [14-21]. These measurements. done correctly with diffuse illumination and detection using integrating spheres, tend to be complicated. Partly for that reason, commercial instruments designed to measure k, s. or related variants such as opacity and color, frequently use a geometry based only on light reflection. This cuts design complexity in half, simplifies calibration, and eliminates the potential need for moving parts. All this leads to lower cost, higher reliability instruments that can perform multiple functions. At the same time, it places restrictions on the range of samples that can be measured accurately.

Measurement of ERIC in recycled pulp is a case in point. TAPPI provisional method T 567 pm-97 [4] recognizes the inability to make a correct diffuse reflectance measurement of ERIC when opacity is above 97.0% at the 950-nm wavelength of interest. In the present study, this value of opacity is reached at ERIC values ranging from about 800 to 900 ppm. The ERIC COV at the limiting opacity ranges from 40% to 80%, dependent on the scattering coefficient. This means that a handsheet producing an ERIC of 243 ppm can, as we observed on retest, also produce a value of 871 ppm. Such a test result encourages the use of an approximate scattering coefficient at opacities lower than 97%. This is contrary to the provisional standard and limits the utility of ERIC to that of a differential measurement.

We have developed and implemented a demonstration test for measuring reflection R and transmission T from a single sheet. The result is used to calculate an ERIC value that is increasingly accurate as opacity increases. For example, recycled newsprint measuring 800 ppm has a standard deviation of about 80 ppm. This level of accuracy facilitates the evaluation of ink removal in recycled pulps by limiting the need for repeat testing. The fact that an assumed scattering value is not needed increases the confidence that changes in fillers and fines are not influencing the result. At 10% accuracy, ERIC values in the literature will have greater credibility because they will be less subject to mill-to-mill variations.

The objective of this paper is to alert the recycling industry to limits in a common test that have not received much attention in recent years and to show a feasible alternative

for going beyond those limits. In the future. the Kubelka-Munk inverse solutions for *k* and *s* (Eqs. (1) or (6) and (7)) may be replaced by software such as DORT2002 [24—26]. This software exchanges the two-flux Kubelka-Munk model with a many-flux model that can he adapted to experimental setups like that of Figure 2. As a result, it may not be necessary to augment setups with costly hardware to get acceptable ERIC measurements. We suggest that refinement of the *RT* method developed here deserves incorporation into methods and provisional methods such as T567 pm-97. It may prove useful whenever diffuse reflection geometries are limited because of high sample opacities.

APPENDIX

Precision Analysis

We conducted mathematical precision analyses of the RT method (Eq. (7)), the R_0R_∞ method (Eq. (1)) and the $\bar{s}R_\infty$ method (Eq. (8)) for ERIC measurements using the following variance (σ^2) estimation equations:

For the *RT* method,

$$10^{-4}\left(\frac{m^2/kg}{ppm}\right)^2\sigma^2(ERIC)=\sigma^2(k)=\left(\frac{\partial k}{\partial R}\right)^2\sigma^2(R)+\left(\frac{\partial k}{\partial T}\right)^2\sigma^2(T) \quad \text{(A1)}$$

For the R_0R_∞ method,

$$10^{-4}\left(\frac{m^2/kg}{ppm}\right)^2\sigma^2(ERIC)=\sigma^2(k)=\left(\frac{\partial k}{\partial R_\infty}\right)^2\sigma^2(R_\infty)+\left(\frac{\partial k}{\partial R_0}\right)^2\sigma^2(R_0) \quad \text{(A2)}$$

For the $\bar{s}R_\infty$ method,

$$10^{-4}\left(\frac{m^2/kg}{ppm}\right)^2\sigma^2(ERIC)=\sigma^2(k)=\left(\frac{\partial k}{\partial \bar{s}}\right)^2\sigma^2(\bar{s})+\left(\frac{\partial k}{\partial R_\infty}\right)^2\sigma^2(R_\infty) \quad \text{(A3)}$$

Once the variance of ERIC is calculated, the COV can be calculated as

$$COV(ERIC)=100\%\times\sigma(ERIC)/ERIC \quad \text{(A4)}$$

This is the function plotted in Figure 4. Since the variances of the experimental variables are known from the data. all that is needed are expressions for the partial derivatives in Equations (A1)-(A3). A requirement is that the experimental variables are independent. However, in an opaque sheet there is a strong dependence of the value for R_∞ on the value R_0. In a translucent sheet, there is a strong dependence of the transmission Ton the reflection *R.* We introduce the substitutions for R_0 and *T,*

$$R_0=R_\infty-\Delta R$$
$$T=1-R-A \quad \text{(A5)}$$

with the claim that the new variables ΔR and A are "more nearly independent" than those they replace, at least in high- or low-opacity sheets, respectively. By substituting Equations (A5) into Equations (1) and (7), as appropriate, the partial derivatives $\frac{\partial k}{\partial \Delta R}$ and $\frac{\partial k}{\partial A}$ can be calculated and used in place of $\frac{\partial k}{\partial R_0}$ and $\frac{\partial k}{\partial T}$ in Equations (A1) and (A2). Experimentally determined variances of the new variables are used as well.

Results show reduced variances in ERIC values, leading to reduced coefficients of variation (COV). In the case of the R_0R_∞ method, COVs are reduced across the range of ERIC values, and these reduced COVs are plotted in Figure 4. In the case of the *RT* method, use of the absorption variable A results in lower COVs for ERIC values of 500 ppm or less, but not for higher values. We have plotted the lower of the two calculated COVs at any given ERIC in Figure 4. This may be noted from the sudden slope change in the plotted curves for the RT method occurring at 500 ppm ERIC. The corresponding standard deviations $\sigma(ERIC)$ are plotted as error bars in Figure 3.

Here are formulas for the partial derivatives required in Equations (A1) and (A2) and in similar equations that can be written using the new variables ΔR and A in place of R_0 and *T,* respectively.

***RT* Method**

Introduce the useful substitution,

$$U=\sqrt{\left(1-T^2+R^2\right)^2-4R^2} \quad \text{(A6)}$$

For the variables R and *T,* the partial derivatives are

$$w\frac{\partial k}{\partial R}=-\left\{\frac{2(1-R)}{U}+\frac{2R\left[(1-R)^2-T^2\right]\left[-1-T^2+R^2\right]}{U^3}\right\}\sinh^{-1}\left(\frac{U}{2T}\right)+\frac{2R\left[(1-R)^2-T^2\right]\left[-1-T^2+R^2\right]}{\left(U^2\right)\sqrt{U^2+4T^2}} \quad \text{(A7)}$$

$$w\frac{\partial k}{\partial T}=\frac{2T}{U}\left\{-1+\frac{\left[(1-R)^2-T^2\right]\left[1-T^2+R^2\right]}{U^3}\right\}\sinh^{-1}\left(\frac{U}{2T}\right)-\frac{2T\left[(1-R)^2-T^2\right]\left[\left(1-T^2+R^2\right)+U^2/2T^2\right]}{U^2\sqrt{U^2+4T^2}} \quad \text{(A8)}$$

For the variables R and A, the partial derivatives are

$$w\frac{\partial k}{\partial R}=\frac{2A}{U}\left\{-1+\frac{\left[(1-R)^2-T^2\right](1+T+R)(R-T)}{U^2}\right\}\sinh^{-1}\left(\frac{U}{2T}\right)-\frac{2A\left[(1-R)^2-T^2\right](1+R+T)(R-T)-U^2/2AT}{\left(U^2\right)\sqrt{U^2+4T^2}} \quad \text{(A9)}$$

$$w\frac{\partial k}{\partial A}=\frac{2T}{U}\left\{1-\frac{\left[(1-R)^2-T^2\right]\left(1+R^2-T^2\right)}{U^2}\right\}\sinh^{-1}\left(\frac{U}{2T}\right)+\frac{2T\left[(1-R)^2-T^2\right]\left[\left(1+R^2-T^2\right)+U^2/2T^2\right]}{\left(U^2\right)\sqrt{U^2+4T^2}} \quad \text{(A10)}$$

R_0R_∞ Method

For the variables R_∞ and R_0, the partial derivatives are

$$w\frac{\partial k}{\partial R_\infty}=-\frac{\ln\left(\frac{1-R_0R_\infty}{1-R_0/R_\infty}\right)}{(1+R_\infty)^2}-\frac{1}{2}\frac{R_0}{R_\infty}\frac{(1-R_\infty)(R_\infty{}^2-2R_0R_\infty+1)}{(1+R_\infty)(1-R_0R_\infty)(R_\infty-R_0)} \quad \text{(A11)}$$

$$w\frac{\partial k}{\partial R_0}=\frac{1}{2}\frac{(1-R_\infty)^2}{(1-R_0R_\infty)(R_\infty-R_0)} \quad \text{(A12)}$$

For the variables R_∞ and ΔR, the partial derivatives are

$$w\frac{\partial k}{\partial R_\infty}=-\frac{\ln\left(\frac{1-R_0R_\infty}{\Delta R/R_\infty}\right)}{(1+R_\infty)^2}+\frac{1}{2R_\infty}\frac{(1-R_\infty)}{(1+R_\infty)}\frac{\left(1-2R_0R_\infty-R_\infty{}^2\right)}{(1-R_0R_\infty)} \quad \text{(A13)}$$

$$w\frac{\partial k}{\partial \Delta R}=-\frac{1}{2\Delta R}\frac{(1-R_\infty)}{(1+R_\infty)}\frac{(1-R_\infty)^2}{(1-R_0R_\infty)} \quad \text{(A14)}$$

Based on our experimental data, the average variances to use in Equations (A1) and (A2) are

$\sigma^2(R_\infty) = (4\%\ R_\infty)^2$. $\sigma^2(R_0)=(4\%R_0)^2$,

$\sigma^2(R)= (4\%R)^2$, and $\sigma^2(T) = (5\%T)^2$

Average variances of new variables are

$\sigma^2(\Delta R) = (2.25\%)^2$ and $\sigma^2(A) = (2.1\%)^2$

These values and Equations (1), (7), (A1), (A2) and (A4)-(A14) determine the theoretical curves of Figure 4 for the R_0R_∞ method and the RT method.

sR_∞ Method

From Equations (8), (A3), and (A4), the formula for the COV is

$$COV(ERIC)=100\%\times\sqrt{COV(\bar{s})^2+COV(R_\infty)^2\left(\frac{1+R_\infty}{1-R_\infty}\right)^2} \quad \text{(A15)}$$

The average COV is 10% for 5 [1] and 3.9% for R_∞. Substitution of the inverse of Equation (8) into Equation (AI 5) for R_∞ allows us to add the theoretical curves for the $\bar{s}R_\infty$ method to Figure 4. Of course, when an estimated or default value is used for $\bar{s}$, it doesn't really qualify as a random variable, so this analysis is not rigorous.

LITERATURE CITED

1. Jordan, B.D.; Popson, S.J. Measuring the concentration of residual ink in recycled newsprint, J. Pulp Paper Sci. 20(6):J161(1994).

2. Kubelka, P.; Munk, F. Ein Beitrag zur Optik der Farbanstriche. Z. Tech. Phys. 12:593 (1931).

3. Kubelka, P. New contributions to the optical properties of intensely light scattering materials. Part I, J. Opt. Soc. Am. 38(5):488(1948); Part II, J. Opt. Soc. Am. 44(4):330(1954); also refer to Robinson, J.V. A summary of reflectance equations for applications of the Kubelka-Munk theory to optical properties of paper. Tappi J., 58(10):152(1975).

4. TAPPI. In TAPPI Test Methods, Determination of effective residual ink concentration by infrared reflectance measurement. Provisional Method T 567 pm-97. TAPPI Press (1997).

5. Van den Akker, J.A. Modern aspects of reflectance spectroscopy. W.W. Wendlandt, ed. Plenum Publishing: NewYork, (1968) p. 27.

6. Giertz, H.W. Some optical consequences of the consolidation of paper, Transac. 3rd Fundamental Res. Symp. Cambridge, UK. p. 928. (1965)

7. Olf, H.G. Correspondence between the Kubelka-Munk and the Stokes model of strongly light-scattering materials, Part II: implications, Tappi J., 72(7):159(1989).

8. Van den Akker. J.A. Comments on the correspondence between the Kubelka-Munk and the Stokes model, Tappi J., 73(2):12(1990).

9. Rundlof, M.; Bristow, J.A. A note concerning the interaction between light scattering and light absorption in the application of the Kubelka-Munk equations. J. Pulp Paper Sci. 23(5):J220 (1997).

10. Koukoulas, A.A.; Jordan, B.D. Effect of strong absorption on the Kubelka-Munk scattering coefficient. J. Pulp Paper Sci. 23(5):J224 (1997).

11. Granberg H.; Edstrom, P. Quantification of the intrinsic error of the Kubelka-Munk model caused by strong light absorption. J. Pulp Paper Sci. 29(11):386(2003).

12. Foote, W.J. An investigation of the fundamental scattering and absorption coefficients of dyed handsheets. Paper Trade J. 109(25):31(1939).

13. Nordman, L.; Aaltonen, P.; and Makkonen, T. Relationships between mechanical and optical properties of paper affected by web consolidation, Transac. 3rd Fundamental Res. Symp., Cambridge, UK. p. 909. (1965)

14. Knox, J.M.; Wahren, D. Determination of light scattering coefficient of dark and heavy sheets. Tappi J. 67(8):82 (1984).

15. Pickering, J.W.; Prahl, S.A.; van Wieringen, N.; Beek, J.F.; Sterenborg, H.J.C.M.; van Gemert, M.J.C. Double-integrating-sphere system for measuring the optical properties of tissue. Appl. Optics 32(4):399 (1993).

16. Ripoll, J.; Yessayan, D.; Zacharakis, G.; Ntziachristos, V. Experimental determination of photon propagation in highly absorbing and scattering media. J. Opt. Soc. Am. A, 22: 546 (2005).

17. Burger, T.; Kuhn, J.; Caps, R.; Fricke, J. Quantitative determination of the scattering and absorption coefficients from diffuse reflectance and transmittance measurements: Application to pharmaceutical powders. Appl. Spectroscopy 51(3):309(1997).

18. Tesfamichael, T.: Hoel, A.; Niklasson, G.A.; Wackelgard, E.; Gunde, M.K.; Orel, Z.C. Optical characterizationmethod for black pigments applied to solar-selective absorbing paints. Appl. Optics 40(10):1672 (2001).

19. Egan, W.G.; Hilgeman, T.; Reichman, J. Determination of absorption and scattering coefficients for nonhomogeneous media. 2: Experiment. Appl. Optics 12(8):1816(1973).

20. Boroumand, F.; van der Bergh, H. Quantitative diffuse reflectance and diffuse transmittance infrared spectroscopy of surface-derivatized silica powders. Anal. Chem. 66: 2260 (1994).

21. Nostell, P.; Roos, A. Single beam integrating sphere spectrophotometer for reflectance and transmittance measurements versus angle of incidence in the solar wavelength range on diffuse and specular samples. Review of Scientific Instruments 70(5):2481 (1999).

22. Haynes, R.D. Measuring the summer effect in North American newsprint deinking mills. 5th Research Forum on Recycling, Ottawa, Sept. p. 25 (1999).

23. Haynes, R.D. The impact of the summer effect on ink detachment and removal. Tappi J., 83 (3):56 (2000).

24. Edström, P. Comparison of the DORT2002 radiative transfer solution method and the Kubelka-Munk model. Nordic Pulp and Paper Res. J. 19(3):397 (2004).

25. Edström, P. A Fast and stable solution method for the radiative transform problem. Siam Review 47(3):447 (2005).

26. Granberg, H.; Béland, M.-C. Modelling the angle-dependent light scattering from sheets of pulp fiber fragments. Nordic Pulp and Paper Res. J. 19(3):354 (2004). ■

The use of firm names in this publication is for reader infirmation and does not imply endorsement by the U.S. Department of Agriculture of any product or service.

Manuscript received for review May 22, 2006.

Revised manuscript received and accepted October 11, 2006.